

Rapid ligand-regulated gating kinetics of single inositol 1,4,5-trisphosphate receptor Ca^{2+} release channels

Don-On Daniel Mak¹⁺, John E. Pearson³, King Pan Campion Loong¹, Suman Datta¹,
Marisabel Fernández-Mongil¹ & J. Kevin Foskett^{1,2}

¹Department of Physiology, and ²Department of Cell and Developmental Biology, University of Pennsylvania, Philadelphia, Pennsylvania, USA, and ³Department of Theoretical Biology and Biophysics, Los Alamos National Laboratory, Los Alamos, New Mexico, USA

The ubiquitous inositol 1,4,5-trisphosphate receptor (InsP₃R) intracellular Ca^{2+} release channel is engaged by thousands of plasma membrane receptors to generate Ca^{2+} signals in all cells. Understanding how complex Ca^{2+} signals are generated has been hindered by a lack of information on the kinetic responses of the channel to its primary ligands, InsP₃ and Ca^{2+} , which activate and inhibit channel gating. Here, we describe the kinetic responses of single InsP₃R channels in native endoplasmic reticulum membrane to rapid ligand concentration changes with millisecond resolution, using a new patch-clamp configuration. The kinetics of channel activation and deactivation showed novel Ca^{2+} regulation and unexpected ligand cooperativity. The kinetics of Ca^{2+} -mediated channel inhibition showed the single-channel bases for fundamental Ca^{2+} release events and Ca^{2+} release refractory periods. These results provide new insights into the channel regulatory mechanisms that contribute to complex spatial and temporal features of intracellular Ca^{2+} signals.

Keywords: intracellular signalling; signal transduction; electrophysiology

EMBO reports (2007) 8, 1044–1051. doi:10.1038/sj.embor.7401087

INTRODUCTION

The ubiquitous endoplasmic reticulum (ER)-localized inositol 1,4,5-trisphosphate receptor (InsP₃R) Ca^{2+} channel has a central role in regulating numerous cell physiological processes by modulating cytoplasmic free Ca^{2+} concentration ($[\text{Ca}^{2+}]_i$) through release of Ca^{2+} from the ER lumen in response to production of cytoplasmic InsP₃ caused by extracellular stimuli (Taylor & Richardson, 1991; Berridge, 1993). InsP₃R channels respond

rapidly (on the order of milliseconds; Marchant & Taylor, 1998) to dynamic changes in the concentrations of their primary ligands—cytoplasmic Ca^{2+} and InsP₃ (Foskett *et al*, 2007). However, kinetic information about single InsP₃R channel responses to ligand concentration changes is lacking. Here, we record, for the first time to our knowledge and with millisecond resolution, the responses of single InsP₃R channels in native ER membranes to controlled changes in $[\text{Ca}^{2+}]_i$ and $[\text{InsP}_3]$ using rapid perfusion techniques (Hinkle *et al*, 2003) applied to cytoplasmic-side-out (cyto-out) nuclear membrane patches (Mak *et al*, 2005). The kinetics of activation and deactivation by $[\text{InsP}_3]$ and $[\text{Ca}^{2+}]_i$ changes have shown novel high-affinity inhibitory Ca^{2+} binding and unexpected cooperativity between InsP₃ and Ca^{2+} . Such ligand regulation has not previously been accounted for in most quantitative models of InsP₃-mediated Ca^{2+} signalling (Swillens *et al*, 1994, 1998; Tang *et al*, 1996; Falcke *et al*, 2000; Fraiman & Dawson, 2004; Sneyd & Falcke, 2005). The kinetics of Ca^{2+} -mediated inhibition have now shown the single-channel bases for fundamental Ca^{2+} release events (Berridge, 1997) and Ca^{2+} release refractory periods (Fraiman *et al*, 2006). This study provides new insights into the channel regulatory mechanisms (Foskett *et al*, 2007) that contribute to complex spatial and temporal features of intracellular Ca^{2+} signals (Putney & Bird, 1993).

RESULTS AND DISCUSSION

Channel activation and deactivation kinetics

Single-channel gating of homo-tetrameric InsP₃R channels in native ER membranes was studied by applying patch-clamp techniques to outer membranes of nuclei isolated from Sf9 cells (Ionescu *et al*, 2006). In the nucleus-attached configuration, with the cytoplasmic aspect of the channel containing the binding sites for InsP₃ and Ca^{2+} facing the pipette solution (Fig 1A), InsP₃R channel activities were observed in the current traces (Fig 1D) when the pipette solution contained activating ligand concentrations— $2\ \mu\text{M}$ Ca^{2+} and $10\ \mu\text{M}$ InsP₃ (Ionescu *et al*, 2006). In excised nuclear membrane patches in the cyto-out configuration (Fig 1B), achieved here for the first time to our knowledge, InsP₃R channels were not observed when the local perfusion solution lacked InsP₃, but their presence was verified by observation of

¹Department of Physiology, and

²Department of Cell and Developmental Biology, University of Pennsylvania, Philadelphia, Pennsylvania 19104, USA

³Department of Theoretical Biology and Biophysics, Los Alamos National Laboratory, Los Alamos, New Mexico 87545, USA

*Corresponding author: Tel: +1 215 898 0468; Fax: +1 215 573 6808;

E-mail: dmak@mail.med.upenn.edu

Received 27 April 2007; revised 20 August 2007; accepted 31 August 2007;
published online 12 October 2007

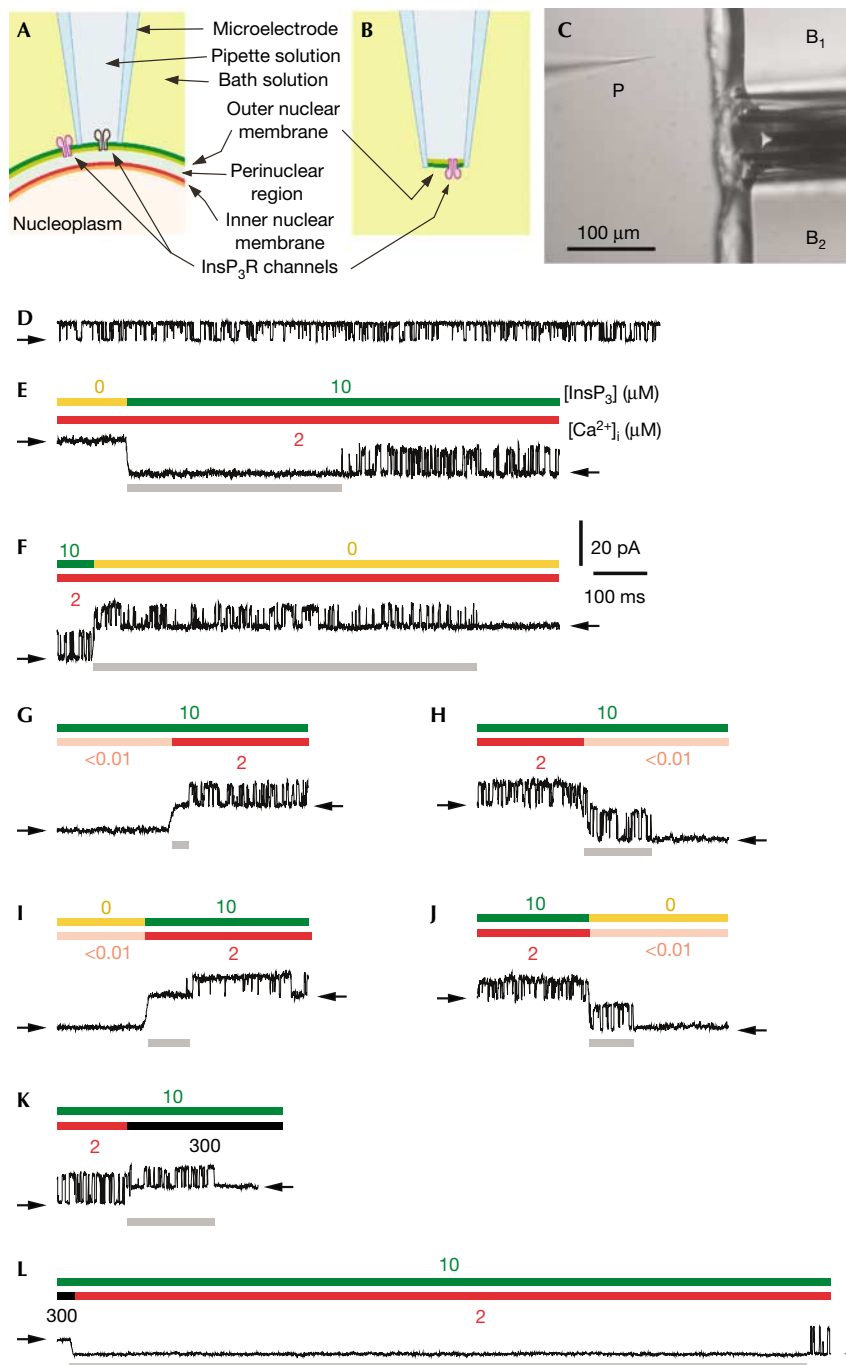


Fig 1 | Nuclear patch-clamp studies of single InsP_3 R channel responses to ligand concentration changes using rapid perfusion techniques applied to cyto-out membrane patches. (A,B) Schematic diagrams illustrating orientation of InsP_3 R channels in nucleus-attached and excised cyto-out configurations, respectively. In the nucleus-attached configuration, the cytoplasmic side of InsP_3 R channels (black) faces the pipette solution. When the cyto-out configuration is obtained, the cytoplasmic side of different InsP_3 R channels (purple) faces the bath solution. (C) Micrograph showing experimental set-up for rapid perfusion. B₁ and B₂ are square glass barrels used to deliver different bath solutions, to which the InsP_3 R channels in the cyto-out nuclear membrane patch at the tip of the micropipette P were alternately exposed. (D) Single-channel current trace showing InsP_3 R channel activity with 10 μM InsP_3 and 2 μM $[\text{Ca}^{2+}]_i$ in the pipette solution in the nucleus-attached configuration. Closed-channel baseline current levels are indicated by arrows in all current traces. (E–L) Single-channel current traces from cyto-out patches showing the responses of InsP_3 R channels to abrupt changes in ligand concentrations, indicated by coloured bars above the traces. Ligand concentrations were changed by switching the perfusing bath solutions, which also caused a change in the level of the closed-channel baseline current because of the different $[\text{KCl}]$ in the perfusing solutions (supplementary information online). This allowed the time course of the perfusing solution switch to be monitored. Response latencies are denoted by grey bars below the traces. Cyto-out, cytoplasmic-side-out; InsP_3 R, inositol 1,4,5-trisphosphate receptor.

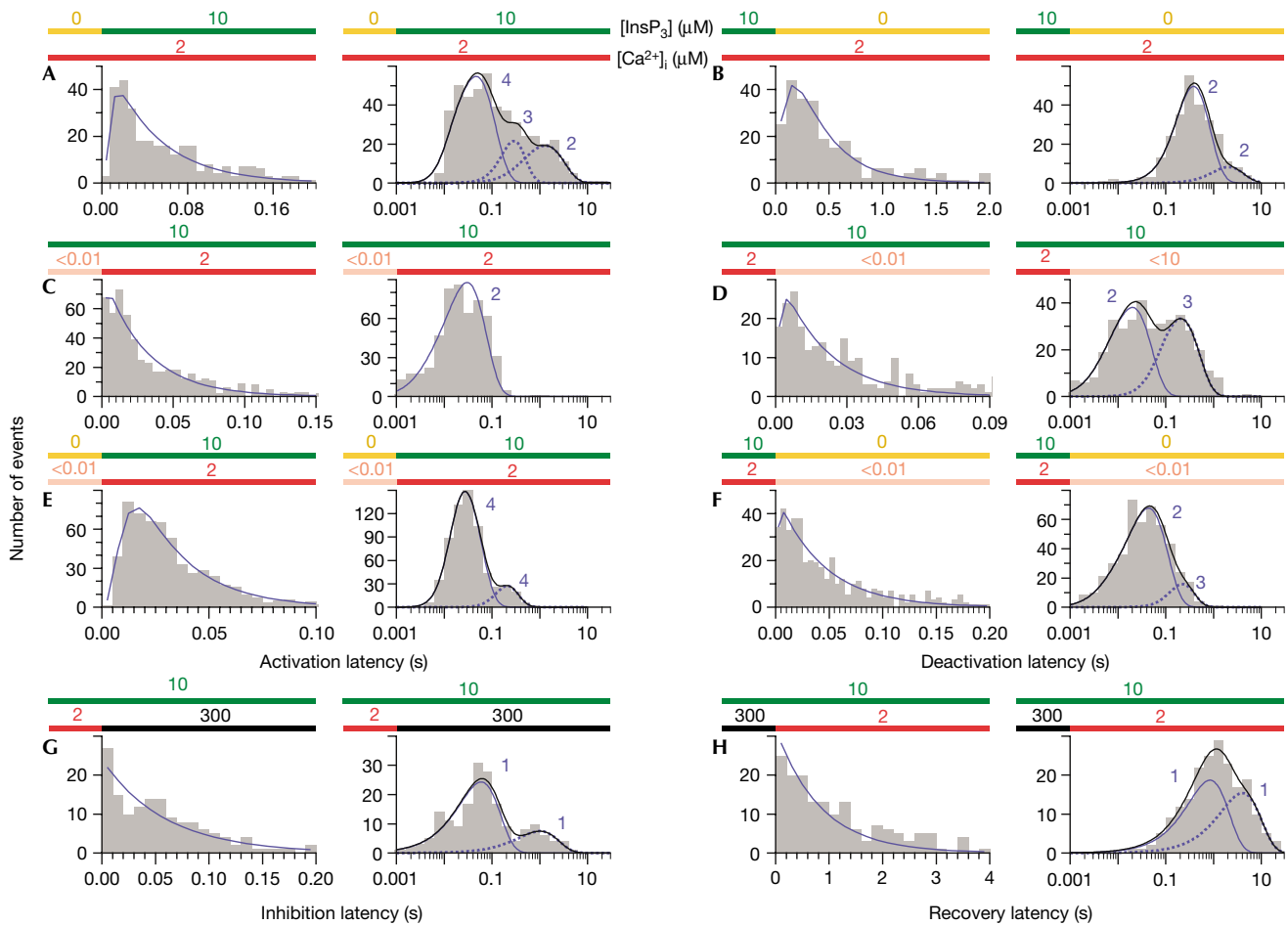


Fig 2 | Latency histograms of InsP₃R channels responding to changes in [InsP₃] and [Ca²⁺]_i. [InsP₃] and [Ca²⁺]_i are denoted by the coloured bars above each histogram. For each type of ligand concentration change investigated, both the linearly binned histogram (left) covering a limited latency range and the logarithmically binned histogram (right) showing the complete range of latencies over all times are shown. In each logarithmically binned histogram, each blue curve is the theoretical fit generated using one linear Markov chain scheme with the tabulated number of functionally indistinguishable conformations (supplementary information online). The black curve is the sum of the theoretical fits if several linear Markov chains were required. In each linearly binned histogram, the blue continuous curve is evaluated using the fastest linear Markov chain scheme and therefore is equivalent to the blue continuous curve in the corresponding logarithmically binned histogram. The range of the x-axis was selected so that the histogram includes at least 95% of the events described by the fastest linear Markov chain scheme. InsP₃R, inositol 1,4,5-trisphosphate receptor.

channel activities (Fig 1E) when the patches were perfused with a solution containing 10 μM InsP₃ and 2 μM Ca²⁺ (Fig 1C).

We first explored the kinetic responses of the channel to rapid changes in [InsP₃]. The mean activation latency in response to a step change of [InsP₃] from 0 to 10 μM in the constant presence of optimal (2 μM) [Ca²⁺]_i was 500 ± 60 ms (Fig 1E; number of solution switches (*n*) = 458; number of cyto-out patches used (*N*) = 14). Because this and all other activation and deactivation latencies showed non-gaussian distributions (Fig 2), non-parametric statistics were used in latency analyses (supplementary information online). A shorter (*P* = 0.002) but still large latency (350 ± 40 ms, *n* = 168, *N* = 4) was observed in response to a step change of [InsP₃] from 0 to 100 μM, indicating that InsP₃ binding and subsequent conformation changes required for channel opening both contribute significantly to the total activation latency. The mean deactivation latency in response to rapidly dropping [InsP₃]

from 10 to 0 μM in the constant presence of optimal [Ca²⁺]_i (690 ± 50 ms; Fig 1F, *n* = 260, *N* = 14) was similar (*P* = 0.06) to that in response to [InsP₃] dropping from 100 μM (700 ± 70 ms, *n* = 123, *N* = 4), as expected. The latency of channel activation by InsP₃ in the presence of 2 μM cytoplasmic Ca²⁺ (Ca²⁺_i) is long compared with those observed for other ligand-activated channels in excitable cells (on the order of microseconds; Maconochie *et al*, 1994). It is also long compared with the latency of Ca²⁺ release resulting from the [InsP₃] jump owing to photolysis of caged InsP₃ in cells (Khodakhah & Ogden, 1995; Parker *et al*, 1996), or rapid perfusion of permeabilized cells or microsomes (Dufour *et al*, 1997). This is not surprising because in such experiments, the latency of Ca²⁺ release through a population of InsP₃R channels was observed. In a system with a large number of InsP₃R channels, the latency to first Ca²⁺ release will be significantly shorter than the activation latency for single InsP₃R channels in response to the

same ligand concentration change (supplementary information online). Furthermore, the non-gaussian distribution of single-channel InsP_3 activation latency (Fig 2A) means that most of the InsP_3 activation latencies observed were shorter than 60 ms even though the mean latency was 500 ms (discussed further in the supplementary information online).

We next explored the kinetics of Ca^{2+} regulation by applying rapid $[\text{Ca}^{2+}]_i$ jumps in the continuous presence of a saturating concentration (10 μM) of InsP_3 . Channel activation by a jump from low (<10 nM) to optimal (2 μM) $[\text{Ca}^{2+}]_i$ had a mean latency of 40 ± 3 ms (Fig 1G, $n=532$, $N=11$), an order of magnitude faster than the response to InsP_3 activation ($P \ll 0.001$). The latency for $[\text{Ca}^{2+}]_i$ jumping to 300 μM was shorter ($P \ll 0.001$) but detectable (24 ± 6 ms, $n=94$, $N=3$), indicating that Ca^{2+} binding and subsequent conformation changes contribute appreciably to the Ca^{2+} activation latency. Channel deactivation when Ca^{2+} was returned to <10 nM had a mean latency of 160 ± 20 ms (Fig 1H, $n=376$, $N=11$), also significantly faster than channel deactivation owing to removal of InsP_3 ($P \ll 0.001$). These results show that InsP_3 -bound channels respond rapidly to changes in $[\text{Ca}^{2+}]_i$, a property ideally suited for Ca^{2+} -induced Ca^{2+} release (CICR) to couple InsP_3R channels in Ca^{2+} signalling (Berridge, 1997).

Remarkably, the mean activation latency in response to simultaneous jumps of $[\text{InsP}_3]$ (from 0 to 10 μM) and $[\text{Ca}^{2+}]_i$ (from <10 nM to 2 μM) was 59 ± 4 ms (Fig 1I, $n=638$, $N=7$)—much shorter than that for InsP_3 activation in the continuous presence of optimal $[\text{Ca}^{2+}]_i$ ($P \ll 0.001$) and comparable with the latency for Ca^{2+} activation in the continuous presence of saturating $[\text{InsP}_3]$. If InsP_3 binding was required before Ca^{2+} can bind, then the activation latency for a simultaneous jump of the two ligands should be comparable with that for InsP_3 in the presence of optimal $[\text{Ca}^{2+}]_i$. These results indicate that there is no requirement for strict sequential InsP_3 and Ca^{2+} binding to activate the channel, invalidating the assumption used in many models that Ca^{2+} can only bind to InsP_3 -bound channels (Tang *et al*, 1996; Marchant & Taylor, 1997; Sneyd & Falcke, 2005). The activation latencies observed here are also incompatible with the independent binding of InsP_3 and Ca^{2+} to activate the channel that is assumed in many other models (Swillens *et al*, 1994, 1998; Tang *et al*, 1996; Hirose *et al*, 1998; Fraiman & Dawson, 2004; Sneyd & Falcke, 2005), because independence predicts that the activation latency for simultaneous $[\text{InsP}_3]$ and $[\text{Ca}^{2+}]_i$ jumps should be longer than the activation latencies for individual $[\text{InsP}_3]$ or $[\text{Ca}^{2+}]_i$ jumps. Instead, the kinetic data are consistent with an unexpected negative cooperative interference, in which high-affinity Ca^{2+} binding to a channel not bound to InsP_3 retards subsequent activation of the channel by InsP_3 .

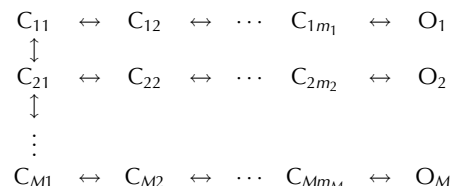
The mean deactivation latency of 69 ± 5 ms for simultaneous removal of InsP_3 (from 10 μM to 0) and Ca^{2+} (from 2 μM to <10 nM) (Fig 1J, $n=458$, $N=7$) was significantly shorter than the deactivation latencies for removal of either InsP_3 ($P \ll 0.001$) or Ca^{2+} ($P=0.002$) alone. This result implies that unbinding of InsP_3 and Ca^{2+} from the InsP_3R is neither sequential nor independent.

Channel activation and deactivation latency distributions

The distributions of InsP_3R channel activation and deactivation latencies showed distinct deficits of short latencies (linearly binned histograms in Fig 2A–F) when compared with a single exponential distribution, similar to those observed during activation

of voltage-gated channels (Patlak & Horn, 1982; Hoshi *et al*, 1994). Such activation latency deficits can be well accounted for by a linear Markov chain scheme connecting C_1 —the closed inactive conformation adopted by the channel before the ligand concentration change—to O —the first open conformation adopted by the channel after the jump in ligand concentration—through one or more intervening closed conformations: $C_1 \leftrightarrow C_2 \leftrightarrow \dots \leftrightarrow C_m \leftrightarrow O$, where $m (\geq 2)$ is the total number of functionally indistinguishable closed conformations in the chain. The deficits of short deactivation latencies can be similarly accounted for by linear Markov chain schemes connecting the initial active open channel conformation to the first inactive closed conformation through several intervening, functionally indistinguishable active conformations (Fig 2; supplementary information online).

The logarithmically binned histogram (Sigworth & Sine, 1987) showing the latency distribution over all timescales of a channel activation or deactivation process described by a linear Markov chain scheme has a peak shape with a single maximum at the dominant time constant. This peak becomes narrower as the number of functionally indistinguishable conformations (m) present in the linear chain increases. However, logarithmically binned histograms of most InsP_3R channel activation and deactivation latencies show multiple maxima or broad shapes that cannot be described with a single linear Markov chain (Fig 2A,B,D–F). These can be satisfactorily described by branched Markov chain schemes such as the one shown below:



in which the channel responding to the ligand concentration change passes through M conformation transition pathways, each corresponding to a linear Markov chain that generates a single peak in the logarithmically binned latency histogram (Fig 2; supplementary information online).

Kinetic schemes accounting for channel latencies

The observed response latencies for single InsP_3R channels point to complex and seemingly paradoxical interactions between InsP_3 and Ca^{2+} activation of the channel. The long activation latencies in response to jumps in $[\text{InsP}_3]$ in the constant presence of optimal $[\text{Ca}^{2+}]_i$ compared with the activation latencies in response to simultaneous jumps in $[\text{InsP}_3]$ and $[\text{Ca}^{2+}]_i$ indicate that Ca^{2+} can bind with high affinity to the channel in the absence of InsP_3 . However, unlike the high-affinity Ca^{2+} binding that activates the channel along with InsP_3 binding that has been established from steady-state studies (Foskett *et al*, 2007), this Ca^{2+} binding interferes negatively with the activation of the channel by InsP_3 . It does this by predisposing the channel to activate through slower conformation transition pathways or by reducing the rate of channel activation through available conformation transition pathways in the branched Markov chain scheme (cf. Fig 2A,E).

Conversely, the significantly more rapid deactivation of the channel in response to simultaneous drops in $[\text{InsP}_3]$ and $[\text{Ca}^{2+}]_i$ compared with channel deactivation caused by drops in either $[\text{InsP}_3]$ or $[\text{Ca}^{2+}]_i$ alone indicates that the InsP_3 and the

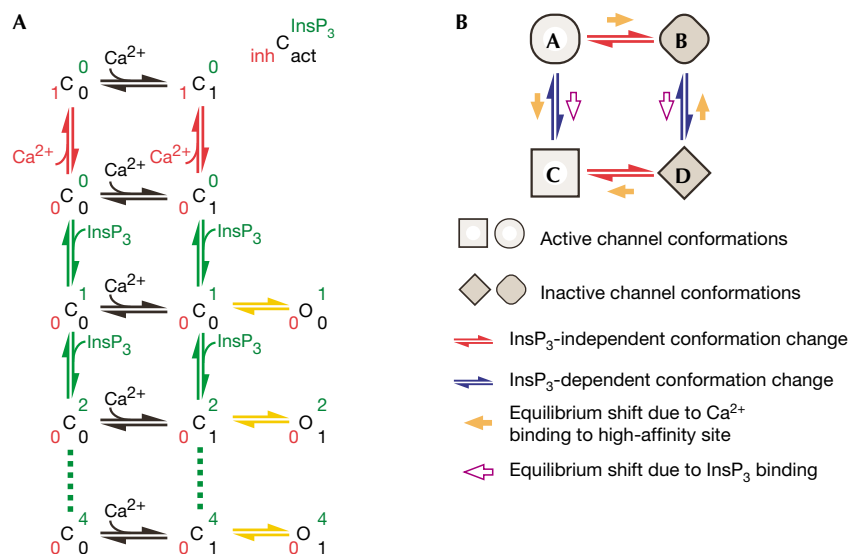


Fig 3 | Kinetic schemes accounting for the observed InsP_3R channel response latencies. **(A)** A qualitative model stipulating distinct high-affinity inhibitory and activating Ca^{2+} sites in each InsP_3R channel. C and O represent closed inactive and active channel conformations. Channel conformations with different ligand binding states are explicitly shown in the scheme by superscript and subscript numbers in different colours: number of occupied high-affinity Ca^{2+} inhibitory sites in red, occupied high-affinity activating Ca^{2+} sites in black and occupied InsP_3 sites in green (as indicated by the key at the top right). Ligand binding and dissociation are indicated by arrows: InsP_3 binding in green, Ca^{2+} binding to inhibitory sites in red and Ca^{2+} binding to activating sites in black. Yellow arrows represent conformation changes. Because the channel is a tetrameric unit, more than one Ca^{2+} can bind to either the activating or inhibitory sites. Those ligand-binding states are not shown in the scheme for clarity. Multiple InsP_3 binding to the channel (dashed lines) is shown to demonstrate that the scheme can accommodate branched Markov chains. **(B)** A qualitative allosteric model stipulating only one kind of high-affinity Ca^{2+} site in an InsP_3R channel. Occupation of the InsP_3 binding sites causes the channel to adopt the C and D conformations instead of the A and B conformations, so that Ca^{2+} binding to the high-affinity Ca^{2+} site becomes activating instead of inhibitory. Unlike **(A)**, only conformation changes are shown in this kinetic scheme. InsP_3 and Ca^{2+} binding to the channel, and the ligand-binding state of the channel conformations are omitted for clarity.

high-affinity Ca^{2+} sites have positive cooperative coupling in an activated channel. Occupation of the InsP_3 or Ca^{2+} sites causes the channel to deactivate through slower conformation transition pathways in the branched Markov chain (cf. Fig 2B,D,F), thereby stabilizing the channel in active conformations.

Fig 3A depicts a kinetic scheme that can account for these observations qualitatively, assuming that the high-affinity inhibitory Ca^{2+} sites are distinct from the high-affinity activating Ca^{2+} sites. Ca^{2+} binding to these inhibitory Ca^{2+} sites precludes InsP_3 binding to the channel, and vice versa. Pre-exposure to optimal $[\text{Ca}^{2+}]_i$ in the absence of InsP_3 retards InsP_3 activation of the channel because InsP_3 cannot bind to the channel until Ca^{2+} dissociates from the inhibitory sites, even after the jump in $[\text{InsP}_3]$. In this scheme, the activating Ca^{2+} sites and the InsP_3 sites show a positive allosteric interaction in an active channel. This is a result of the different channel deactivation rates by various pathways in the branched Markov chain generated by multiple InsP_3 and Ca^{2+} binding to the tetrameric channels, shown partly in Fig 3A.

Alternatively, a model stipulating that only one high-affinity Ca^{2+} site is present in each InsP_3R monomer is also qualitatively consistent with all the kinetic responses observed here. The model, a simplified version of a quantitative model proposed to account for steady-state InsP_3 and Ca^{2+}_i regulation of channel activity (Mak et al, 2003), assumes only basic allosteric interactions between the two ligands that arise solely from preferential binding of InsP_3 and Ca^{2+} to various channel conformations. In its

simplest form (Fig 3B), the model hypothesizes that the channel can adopt four different conformations. In the absence of InsP_3 , it is energetically favourable for the channel to adopt two conformations, one active (A) and one inactive (B), with Ca^{2+} binding to the high-affinity sites stabilizing the inactive B conformation. Thus, in the absence of InsP_3 , the high-affinity Ca^{2+} sites are actually inhibitory. InsP_3 binding to the channel energetically stabilizes the other two conformations, also one active (C) and one inactive (D). Ca^{2+} binding to the high-affinity sites stabilizes the active C conformation relative to the inactive D conformation. Consequently, the high-affinity Ca^{2+} sites are activating when the channel is InsP_3 -bound. Thus, because of the different relative affinities of the high-affinity Ca^{2+} sites in the four channel conformations, InsP_3 binding to the channel changes the nature of the high-affinity Ca^{2+} binding sites from inhibitory to activating. This transformative effect of InsP_3 on the nature of the high-affinity Ca^{2+} binding sites can account for the seemingly paradoxical channel response latencies measured here. Because Ca^{2+} binding to the high-affinity sites in the absence of InsP_3 stabilizes the inactive B conformation, which has low affinity for InsP_3 , pre-exposure of the channel to $2\ \mu\text{M}\ \text{Ca}^{2+}_i$ slows down binding of InsP_3 to the channel and consequent activation kinetics compared with activation by simultaneous $[\text{Ca}^{2+}]_i$ and $[\text{InsP}_3]$ jumps. Conversely, occupation of the high-affinity Ca^{2+} and InsP_3 sites stabilizes an active channel in the C conformation with high affinity for InsP_3 and Ca^{2+} . This accounts for the shorter mean latency for

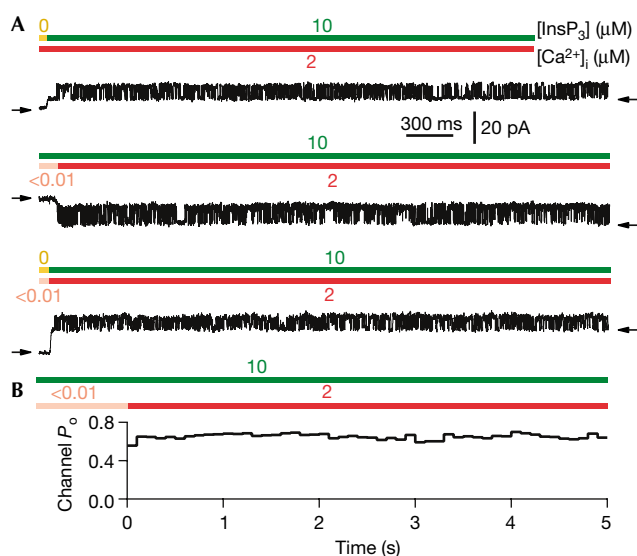


Fig 4 | Steady level of InsP_3R channel activity observed after channel activation by abrupt jumps in ligand concentration. (A) Current traces of InsP_3R channels after activation by step change in $[\text{InsP}_3]$ (top), $[\text{Ca}^{2+}]_i$ (middle) and both simultaneously (bottom). (B) Averaged time course of P_o (in 0.1 s bins) of one InsP_3R channel after step change of $[\text{Ca}^{2+}]_i$ at $t=0$ in one membrane patch. A total of 72 $[\text{Ca}^{2+}]_i$ jumps were averaged. InsP_3R , inositol 1,4,5-trisphosphate receptor.

deactivation by simultaneous removal of InsP_3 and Ca^{2+} , compared with that owing to removal of either Ca^{2+} or InsP_3 alone. The model hypothesizes that the channel can adopt the different conformations in any ligand-binding state, and InsP_3 binding and Ca^{2+} binding regulate channel activity by affecting the probability of the channel being in various conformations. Thus, active and inactive conformations are connected by many branched pathways through various ligand binding and conformation changes.

Channel activity level after activation

It has been speculated that spontaneous changes in channel activity after the initial activation might account for biphasic Ca^{2+} release kinetics and graded release of Ca^{2+} from intracellular stores in response to incremental levels of stimulation (Muallem *et al*, 1989; Meyer & Stryer, 1990; Marchant & Taylor, 1998). However, no change in single-channel P_o was observed after the InsP_3R was activated by jumps in $[\text{InsP}_3]$, $[\text{Ca}^{2+}]_i$ or both simultaneously (Fig 4). Thus, behaviours akin to ‘adaptation’ observed in the ryanodine receptor (Fill *et al*, 2000) are unlikely to account for InsP_3R -mediated graded release of Ca^{2+} .

Channel inhibition and recovery kinetics

The steady-state gating activity of the InsP_3R is biphasically regulated by $[\text{Ca}^{2+}]_i$, indicating that the channel also has low-affinity inhibitory Ca^{2+} binding sites (Foskett *et al*, 2007). Ca^{2+} inhibition can provide a negative feedback mechanism to either terminate or prevent Ca^{2+} release as the local $[\text{Ca}^{2+}]_i$ is raised by InsP_3R -mediated Ca^{2+} release. This can have significant roles in generating Ca^{2+} spikes and oscillations, and in creating highly localized Ca^{2+} signals in subcellular compartments by preventing runaway Ca^{2+} release due to CICR. Switching $[\text{Ca}^{2+}]_i$ from 2 μM

(optimal) to 300 μM (inhibitory; Ionescu *et al*, 2006) in the presence of 10 μM InsP_3 inhibited channel gating (Fig 1K). This shows that InsP_3 binding does not render the low-affinity inhibitory Ca^{2+} sites inaccessible for Ca^{2+} binding, disproving previous claims (Adkins & Taylor, 1999). The mean latency for Ca^{2+} inhibition (290 ± 40 ms, $n=186$, $N=7$) was substantially longer than that for Ca^{2+} activation ($P \ll 0.001$).

The mean latency for channel recovery from Ca^{2+} inhibition was 2.4 ± 0.2 s (Fig 1L, $n=197$, $N=7$). This remarkably long latency defines a refractory period between successive Ca^{2+} release events mediated by the same InsP_3R channel or channel cluster. A refractory period has been invoked to account for mutual annihilation of colliding intracellular Ca^{2+} waves (Lechleiter *et al*, 1991) and the periodicity of Ca^{2+} oscillations (Parker & Ivorra, 1990), but its molecular basis has remained unknown. The observed latency is in quantitative agreement with the mean refractory periods (~ 2.5 s) between two successive spontaneous InsP_3R -mediated elementary Ca^{2+} release events (puffs) observed in the presence of saturating $[\text{InsP}_3]$ (Fraiman *et al*, 2006). This result indicates that the latency for channel recovery from Ca^{2+} inhibition, rather than other mechanisms such as lingering high $[\text{Ca}^{2+}]_i$ in the vicinity of the Ca^{2+} release sites after a Ca^{2+} release event, is responsible for the refractory behaviour of Ca^{2+} release sites observed *in vivo* (Ilyin & Parker, 1994).

In contrast to the lack of short latencies in channel activation and deactivation, latency distributions of channel inhibition by Ca^{2+} and recovery (Fig 2G,H) have no appreciable deficits of short events. This indicates that the active conformation adopted by the channel in optimal (2 μM) $[\text{Ca}^{2+}]_i$ is in effect connected directly to an inactive conformation through the binding of a single Ca^{2+} to one inhibitory low-affinity site. More remarkably, even in the presence of 300 μM Ca^{2+} , the channel is in an inactive conformation that is connected directly to an active conformation through the dissociation of a single Ca^{2+} , despite the tetrameric channel structure with possibly four equivalent inhibitory Ca^{2+} sites. Thus, Ca^{2+} inhibition of the channel can be described by a simple two-state kinetic scheme: $\text{O} \leftrightarrow \text{I}$. This is consistent with the observation that Ca^{2+} inhibition of steady-state gating of Sf9 InsP_3R in the presence of 10 μM InsP_3 showed a Hill coefficient of approximately 1 (Ionescu *et al*, 2006). It is possible that the multiple Ca^{2+} inhibitory sites have strong negative cooperativity so that binding of Ca^{2+} to one of them prevents Ca^{2+} from binding to the remaining vacant sites.

Kinetics of single-channel Ca^{2+} release burst

In cells, Ca^{2+} released by an individual channel raises $[\text{Ca}^{2+}]_i$ to inhibitory (~ 100 μM) levels in the microdomain surrounding it. Our kinetic results predict that this Ca^{2+} will feed back to inhibit it and terminate release after a burst of activity. $[\text{Ca}^{2+}]_i$ jumps from low sub-activating (<10 nM) levels directly to inhibitory (300 μM) levels in the presence of 10 μM InsP_3 produced just such a burst of channel activity. This is due to Ca^{2+} first binding to the high-affinity sites to activate the channel before the low-affinity inhibitory sites become occupied (Fig 5A). Mean activation and inhibition latencies of channel activity bursts were 24 ± 6 ms (Fig 5B, $n=94$, $N=3$) and 470 ± 90 ms (Fig 5C, $n=70$, $N=3$), respectively. The mean single-channel burst duration was 470 ± 100 ms (Fig 5D, $n=50$, $N=3$). The time course of these channel activity bursts represents the kinetics of the fundamental

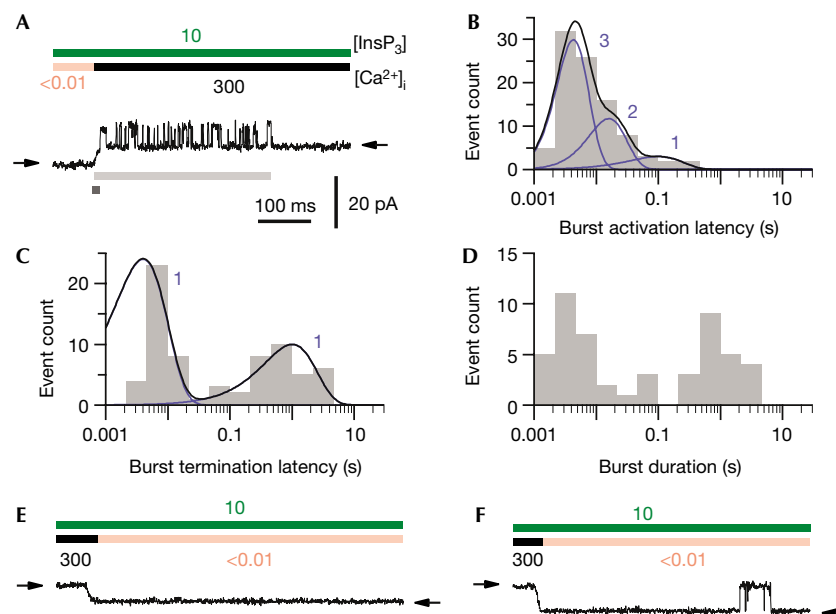


Fig 5 | Kinetics of InsP₃R channel activity bursts in response to [Ca²⁺]_i changes between sub-activating (<10 nM) and inhibitory (300 μM) levels in the presence of 10 μM InsP₃. (A) A typical current trace of InsP₃R channel activity burst in response to [Ca²⁺]_i increasing from <10 nM to 300 μM. The burst activation and termination latencies are denoted by the dark and light grey bars, respectively. (B–D) Logarithmically binned histograms of burst activation and termination latencies, and burst durations, respectively. The latency distributions were fitted (black curves) using more than one linear Markov chain schemes (blue curves). The number of functionally indistinguishable conformations in each scheme is tabulated next to the corresponding blue curve. Short latencies of burst termination were not observed in (C) because when Ca²⁺ binds rapidly to the inhibitory sites before it binds to the activating sites, no channel activity follows. (E,F) Typical current traces showing different InsP₃R channel responses to rapid decrease in [Ca²⁺]_i from 300 μM to <10 nM.

Ca²⁺ release event—the basic building block from which local concerted Ca²⁺ release by clusters of InsP₃R channels (puffs) and global propagating InsP₃R-mediated Ca²⁺ signals (waves) are generated through CICR (Berridge, 1997).

A considerable fraction (9 out of 103) of [Ca²⁺]_i jumps from <10 nM to 300 μM failed to generate a burst (although [Ca²⁺]_i jumps before and after those jumps did generate bursts), substantially greater than that (7 out of 607) for [Ca²⁺]_i jumps from <10 nM to 2 μM. Thus, Ca²⁺ binding to the high-affinity activating sites and low-affinity inhibitory sites is not sequential, and the failure of [Ca²⁺]_i jumps (<10 nM to 300 μM) to generate an activity burst reflects the non-zero probability of Ca²⁺ binding to an inhibitory site before the activating sites becomes occupied. The mean latency for recovery from Ca²⁺ inhibition is over an order of magnitude longer than the mean latency of deactivation by Ca²⁺ removal ($P \ll 0.001$). Therefore during most [Ca²⁺]_i drops (from 300 μM to <10 nM), no channel activity was observed as the channels were deactivated by Ca²⁺ dissociation from the high-affinity activating sites before they recovered from Ca²⁺ inhibition (Fig 5E). However, in 6 out of 94 [Ca²⁺]_i drops, the channel recovered from Ca²⁺ inhibition first, generating a brief burst of activity before it was deactivated by Ca²⁺ unbinding (Fig 5F). This indicates that Ca²⁺ dissociation from the inhibitory and activating sites is also not sequential.

CONCLUSIONS

The rapid kinetic responses of single InsP₃R channels in native ER membranes to [InsP₃] and [Ca²⁺]_i changes observed here have

provided new insights into the molecular mechanisms of channel activation and inhibition by these ligands. These measurements have shown that there is no requirement for sequential InsP₃ and Ca²⁺ binding during channel activation or deactivation, but binding of the two ligands is nevertheless not independent. A complex interaction involving both positive and negative cooperativity exists between InsP₃ and high-affinity Ca²⁺ binding sites, which was not anticipated in most theoretical models of the InsP₃R. The kinetics of high [Ca²⁺]_i inhibition of channel activity have provided insights into the molecular basis of fundamental Ca²⁺-release events and the refractory period that accounts for [Ca²⁺]_i oscillation frequency and wave annihilation. These single-channel kinetic data thus provide novel quantitative details for future construction of realistic models to account for the role of InsP₃R channel kinetics in generating cytoplasmic Ca²⁺ signals (Shuai et al, 2007). The approaches described here can also be used in future studies to define the kinetics of other types of InsP₃R channel regulation, and facilitate better understanding of [Ca²⁺]_i signalling by the ubiquitous InsP₃ pathway.

METHODS

Single-channel patch-clamp studies of InsP₃R channels in a native membrane environment using isolated nuclei from cultured insect *Spodoptera frugiperda* (Sf9) cells were performed in cyto-out excised patch configuration. The cytoplasmic side of the nuclear membrane patch and of any InsP₃R channels therein was exposed to different perfusing solutions containing various ligand concentrations during a continuous patch-clamp recording using a rapid perfusion

set-up. Activation latency is the duration between the solution switch time and the first observed channel opening event in response to the solution switch. Similarly, deactivation latency is the duration between solution switch time and the last observed channel closing. The analysis allows latencies > 5 ms to be clearly and consistently resolved. Current traces from cyto-out membrane patches containing one to several (≤ 10) active InsP₃R channels were selected for latency analysis (supplementary information online).

Supplementary information is available at *EMBO reports* online (<http://www.emboreports.org>).

ACKNOWLEDGEMENTS

We thank P. De Weer, C. Deutsch, F.T. Horrigan, T. Hoshi and E.M. Ostap for comments on the manuscript and W.J. Bruno for help with statistical analysis of the data. This work was supported by National Institutes of Health grants GM074999 to D.-O.D.M., MH059937 to J.K.F. and GM65830 to J.E.P.

REFERENCES

- Adkins CE, Taylor CW (1999) Lateral inhibition of inositol 1,4,5-trisphosphate receptors by cytosolic Ca²⁺. *Curr Biol* **9**: 1115–1118
- Berridge MJ (1993) Inositol trisphosphate and calcium signalling. *Nature* **361**: 315–325
- Berridge MJ (1997) Elementary and global aspects of calcium signalling. *J Physiol* **499**: 291–306
- Dufour JF, Arias IM, Turner TJ (1997) Inositol 1,4,5-trisphosphate and calcium regulate the calcium channel function of the hepatic inositol 1,4,5-trisphosphate receptor. *J Biol Chem* **272**: 2675–2681
- Falcke M, Tsimring L, Levine H (2000) Stochastic spreading of intracellular Ca²⁺ release. *Phys Rev E* **62**: 2636–2643
- Fill M, Zahradnikova A, Villalba-Galea CA, Zahradnik I, Escobar AL, Gyorko S (2000) Ryanodine receptor adaptation. *J Gen Physiol* **116**: 873–882
- Foskett JK, White C, Cheung KH, Mak D-OD (2007) Inositol trisphosphate receptor Ca²⁺ release channels. *Physiol Rev* **87**: 593–658
- Fraiman D, Dawson SP (2004) A model of IP₃ receptor with a luminal calcium binding site: stochastic simulations and analysis. *Cell Calcium* **35**: 403–413
- Fraiman D, Pando B, Dargan S, Parker I, Dawson SP (2006) Analysis of puff dynamics in oocytes: interdependence of puff amplitude and interpuff interval. *Biophys J* **90**: 3897–3907
- Hinkle DJ, Bianchi MT, Macdonald RL (2003) Modifications of a commercial perfusion system for use in ultrafast solution exchange during patch clamp recording. *Biotechniques* **35**: 472–476
- Hirose K, Kadowaki S, Iino M (1998) Allosteric regulation by cytoplasmic Ca²⁺ and IP₃ of the gating of IP₃ receptors in permeabilized guinea-pig vascular smooth muscle cells. *J Physiol* **506**: 407–414
- Hoshi T, Zagotta WN, Aldrich RW (1994) Shaker potassium channel gating. I: transitions near the open state. *J Gen Physiol* **103**: 249–278
- Ilyin V, Parker I (1994) Role of cytosolic Ca²⁺ in inhibition of InsP₃-evoked Ca²⁺ release in *Xenopus* oocytes. *J Physiol* **477**: 503–509
- Ionescu L, Cheung KH, Vais H, Mak D-OD, White C, Foskett JK (2006) Graded recruitment and inactivation of single InsP₃ receptor Ca²⁺-release channels: implications for quantal Ca²⁺ release. *J Physiol* **573**: 645–662
- Khodakhah K, Ogden D (1995) Fast activation and inactivation of inositol trisphosphate-evoked Ca²⁺ release in rat cerebellar Purkinje neurones. *J Physiol* **487**: 343–358
- Lechleiter J, Girard S, Peralta E, Clapham D (1991) Spiral calcium wave propagation and annihilation in *Xenopus laevis* oocytes. *Science* **252**: 123–126
- Maconochie DJ, Zempel JM, Steinbach JH (1994) How quickly can GABA_A receptors open? *Neuron* **12**: 61–71
- Mak D-OD, McBride SM, Foskett JK (2003) Spontaneous channel activity of the inositol 1,4,5-trisphosphate (InsP₃) receptor (InsP₃R). Application of allosteric modeling to calcium and InsP₃ regulation of InsP₃R single-channel gating. *J Gen Physiol* **122**: 583–603
- Mak D-OD, White C, Ionescu L, Foskett JK (2005) Nuclear patch clamp electrophysiology of inositol trisphosphate receptor Ca²⁺ release channels. In *Methods in Calcium Signaling Research*, Putney JW Jr (ed) pp 203–229. Boca Raton, FL, USA: CRC Press
- Marchant JS, Taylor CW (1997) Cooperative activation of IP₃ receptors by sequential binding of IP₃ and Ca²⁺ safeguards against spontaneous activity. *Curr Biol* **7**: 510–518
- Marchant JS, Taylor CW (1998) Rapid activation and partial inactivation of inositol trisphosphate receptors by inositol trisphosphate. *Biochemistry* **37**: 11524–11533
- Meyer T, Stryer L (1990) Transient calcium release induced by successive increments of inositol 1,4,5-trisphosphate. *Proc Natl Acad Sci USA* **87**: 3841–3845
- Muallem S, Pandolfi SJ, Beeker TG (1989) Hormone-evoked calcium release from intracellular stores is a quantal process. *J Biol Chem* **264**: 205–212
- Parker I, Ivorra I (1990) Inhibition by Ca²⁺ of inositol trisphosphate-mediated Ca²⁺ liberation: a possible mechanism for oscillatory release of Ca²⁺. *Proc Natl Acad Sci USA* **87**: 260–264
- Parker I, Yao Y, Ilyin V (1996) Fast kinetics of calcium liberation induced in *Xenopus* oocytes by photoreleased inositol trisphosphate. *Biophys J* **70**: 222–237
- Patlak J, Horn R (1982) Effect of N-bromoacetamide on single sodium-channel currents in excised membrane patches. *J Gen Physiol* **79**: 333–351
- Putney Jr JW, Bird GS (1993) The inositol phosphate–calcium signaling system in nonexcitable cells. *Endocr Rev* **14**: 610–631
- Shuai J, Pearson JE, Foskett JK, Mak D-OD, Parker I (2007) A kinetic model of single and clustered IP₃ receptors in the absence of Ca²⁺ feedback. *Biophys J* **93**: 1151–1162
- Sigworth FJ, Sine SM (1987) Data transformations for improved display and fitting of single-channel dwell time histograms. *Biophys J* **52**: 1047–1054
- Sneyd J, Falcke M (2005) Models of the inositol trisphosphate receptor. *Prog Biophys Mol Biol* **89**: 207–245
- Swillens S, Combettes L, Champeil P (1994) Transient inositol 1,4,5-trisphosphate-induced Ca²⁺ release: a model based on regulatory Ca²⁺-binding sites along the permeation pathway. *Proc Natl Acad Sci USA* **91**: 10074–10078
- Swillens S, Champeil P, Combettes L, Dupont G (1998) Stochastic simulation of a single inositol 1,4,5-trisphosphate-sensitive Ca²⁺ channel reveals repetitive openings during ‘blip-like’ Ca²⁺ transients. *Cell Calcium* **23**: 291–302
- Tang Y, Stephenson JL, Othmer HG (1996) Simplification and analysis of models of calcium dynamics based on IP₃-sensitive calcium channel kinetics. *Biophys J* **70**: 246–263
- Taylor CW, Richardson A (1991) Structure and function of inositol trisphosphate receptors. *Pharmacol Ther* **51**: 97–137